Spectrochimica Acta Part A: Molecular and Biomolecular Spectroscopy 225 (2020) 117476

Contents lists available at ScienceDirect

Spectrochimica Acta Part A: Molecular and Biomolecular Spectroscopy

journal homepage: www.elsevier.com/locate/saa

# Far-infrared terahertz properties of L-cysteine and its hydrochloride monohydrate

Guanhua Ren [a,c], Siqi Zong [c], Zhongjie Zhu [c], Chao Cheng [c], Ligang Chen [a], Lu Zhou [a], Jianbing Zhang [b,c], Liyuan Liu [a], Jiaguang Han [a,*], Hongwei Zhao [b,c,**]

[a] Center for Terahertz Waves and College of Precision Instrument and Optoelectronics Engineering, Tianjin University, and Key Laboratory of Optoelectronics Information and Technology, Ministry of Education, Tianjin 300072, China
[b] Shanghai Advanced Research Institute Zhangjiang Lab, Chinese Academy of Sciences, No.99 Haike Road, Zhangjiang Hi-Tech Park, Pudong Shanghai, Shanghai 201210, China
[c] Shanghai Institute of Applied Physics, Chinese Academy of Sciences, Shanghai 201800, China

ARTICLE INFO

*Article history:*
Received 26 April 2019
Received in revised form 27 July 2019
Accepted 17 August 2019
Available online 19 August 2019

*Keywords:*
L-cysteine
L-cysteine hydrochloride monohydrate
Terahertz spectra

ABSTRACT

As the building blocks of proteins, amino acids serve vital metabolic functions in addition to protein synthesis and thus attract enormous interest. Here we reported the far-infrared optical properties of L-cysteine (Lcys) and its hydrochloride monohydrate (LCHM) characterized by terahertz time-domain spectroscopy. The Lcys and LCHM exhibit quite distinct characteristics in the terahertz region due to diverse collective vibrations of the molecules, which is further confirmed by the solid-state density functional theory (DFT) calculations. The presented studies indicate that the intermolecular hydrogen bonds play a critical role in the far-infrared terahertz response of Lcys and LCHM.



## 1. Introduction

Amino acids are the monomers that polymerize to form proteins and the unique sequence of amino acids in a protein thus constitute its primary structure. As the structure basic unit, amino acids not only fulfill vital roles in protein synthesis but also serve critical metabolic functions. Although proteins in the cells are tremendously versatile, most of them are composed of just 20 different amino acids. All 20 of these building block amino acids share a common core structure, but each one shows distinctive properties due to the different side chains [1]. Among the family of amino acids, L-cysteine ($NH_3^+$–CH($CH_2SH$)–$COO^-$, Lcys) has gathered a great attention on account of its high reactivity and numerous biological functions. It is known that Lcys is a pivotal amino acid in the binding site of the cystic fibrosis transmembrane regulator ion channel which is associated with the devastating effects of cystic fibrosis [2]. Lcys is capable of forming chemical bonds with metal surfaces through its thiol side chain and provides the molecular hook between several biomolecules and metal surfaces [3]. In addition, Lcys also participates in the biosynthesis of coenzyme A and may be essential for infants, the elderly and individuals with certain metabolic diseases [4]. As the hydrochloride salt of Lcys, L-cysteine hydrochloride monohydrate ($NH_3^+$–CH($CH_2SH$)–$COOH\cdot Cl^-\cdot H_2O$, LCHM) is a residue within chloride ion channel proteins associated with disease. LCHM is implicated in the mutations of the CLCNKB (Chloride channel Kb) chloride channel which leads to Bartter's syndrome type III [5]. LCHM is also one of the most efficient known radiation-protection agents [6].

Consider the essential importance of Lcys and its hydrochloride derivatives in modern cells, and hence we have an increasing demand to get to know more basic properties of them, such as the spectral characteristics at various frequency ranges. Different spectroscopic techniques have been devoted to analyze Lcys and its hydrochloride derivatives. Schillinger et al. studied the enantioselectivity of cysteine molecules on Au surface using X-ray photoelectron spectroscopy [7]. Min'kov et al. studied the 600–4000 $cm^{-1}$ infrared (IR) spectra of L-cysteine and DL-cysteine from 333 to 83 K [8]. It shows that IR spectra of L-cysteine and DL-cysteine are substantially different and the differences are considered to be related to the vibrations of $–NH_3^+$, $–COO^-$ and –SH groups involved in hydrogen bond, which may be affected by the temperature. Chapman et al. studied the local environment of chlorine in LCHM using chlorine solid-state Nuclear Magnetic Resonance spectroscopy [9]. Bhagavannarayana et al. studied the vibrational modes and functional groups of single crystal LCHM using Fourier transform (FT) Raman spectroscopy [10], and assigned the weak peak around 200 $cm^{-1}$ to the lattice vibrations in the bulk crystal specimen.

Thus far, though we have obtained some certain spectra information of Lcys and LCHM, we have only a limited knowledge about the far-infrared characteristics of them. Continued interest in this subject is

* Corresponding author.
** Correspondence to: H. Zhao, Shanghai Advanced Research Institute Zhangjiang Lab, Chinese Academy of Sciences, No.99 Haike Road, Zhangjiang Hi-Tech Park, Pudong Shanghai, Shanghai 201210, China.
*E-mail addresses:* jiaghan@tju.edu.cn (J. Han), zhaohongwei@sinap.ac.cn (H. Zhao).

https://doi.org/10.1016/j.saa.2019.117476
1386-1425/

fueled with the development of time-domain terahertz spectroscopy (THz-TDS). Due to its longer wavelength and lower energy, terahertz waves are not ionizing but could probe the low-frequency torsional vibration or rotation energy levels of most molecules without damaging the sample [11]. In particularly, these terahertz spectra are highly sensitive to the conformation and structure of molecules. THz-TDS has been widely applied in molecular studies. Janek et al. studied the microcrystalline clay minerals modified by amino acids using THz-TDS and found that the hectorite intercalated with cysteine has distinct vibrations as dimmer of cysteine molecule [12]. Upadhya et al. studied the vibrational modes of different polycrystalline saccharides, and identified distinct vibrational features as the signatures of inter- and/or intramolecular modes [13]. Kröll et al. studied the sucrose single-crystals and obtained the THz absorption spectra for different polarization orientations of sucrose crystals [14]. Consequently, as a nondestructive data acquisition and coherence detection technology, THz-TDS provides a reliable and unique analytical method to study the characteristics of molecules in the far-infrared frequency region. In this paper, we present a systematic study of far-infrared terahertz properties of Lcys and LCHM by using THz-TDS. The temperature-dependent far-infrared terahertz spectroscopic properties of Lcys and LCHM in the frequency range from 0.5 to 4.0 THz have been characterized. The measured results are analyzed based on the intermolecular vibrational modes of Lcys and LCHM calculated by DFT method.

## 2. Materials and methods

Lcys and LCHM (purities ≥99.0%) were purchased from J&K Co. Ltd. and used without further purification. Then the Lcys and LCHM were respectively mixed with cyclic olefin copolymer powder (COC, purchased from Shanghai Institute of Nuclear Research) in a mass ratio of 1:10 and then pressed them into tablet samples of a diameter of 13 mm and a thickness of around 1.2 mm under a pressure of 2.0 MPa. The used COC powder is as the matrix to ensure that the measurements were made within an optimal absorption range because it has a very low absorption and negligible dispersion at terahertz frequencies [15]. The Lcys and LCHM samples are characterized by broadband (0.5–4.0 THz) THz-TDS (TAS7400TS, Advantest Corporation, Japan). The sample was placed into the THz-TDS system which was purged with dry air to keep the relative humidity under 1% and each spectrum was average of 512 scans with the drying air as the reference.

Low temperature measurements were carried out with a liquid nitrogen flowed cryostat (Specac Ltd. UK, accuracy ±0.5 °C) cell. A series of THz spectra of Lcys and LCHM were recorded in the temperature range of 83–293 K.

Powder X-ray diffraction (PXRD) measurements were performed on Bruker D8 Advance (Cu tube with 1. 1.5406 Å, 40 kV voltage, 40 mA filament emission). The data were collected with a scan ranging from 10° to 90° ($2\theta$) at room temperature.

## 3. Computational method

To understand the experimentally measured terahertz responses of the Lcys and LCHM samples, quantum chemical calculations were performed based on the solid-state DFT using the Cambridge Sequential Total Energy Package (CASTEP) program [16] as a part of Materials Studio package from Accelrys. The results were obtained for the crystalline state within the generalized gradient approximation (GGA) at Perdew-Burke-Ernzerhof (PBE) correlation functional [17], using Grimme's DFT-D2 dispersion-corrected method for DFT-D correction and norm-conserving pseudopotential as implemented in CASTEP [18–21]. During the calculations, the plane-wave cutoff energy was set as 830 eV, Brillouin zone sampling of electronic states were performed on $2 \times 1 \times 3$ and $3 \times 2 \times 1$ Monkhorst-Pack grid for Lcys and LCHM, respectively. The total energy was converged to $5.0 \times 10^{-6}$ eV/atom and the maximum forces between atoms were <0.01 eV/Å. Vibration modes were analyzed using vibrational analysis tool packaged in Materials Studio, which could obtain the vibrational frequencies and intensities of molecules from Hessian matrix and atomic polar tensors respectively.

## 4. Result and discussion

### 4.1. THz absorption spectra of Lcys and LCHM

The transmitted terahertz through both the sample and the reference were measured and the terahertz power absorption could be extracted through the ratio between the spectra of the sample and the reference [22]. The frequency-dependent power absorption coefficients of the measured Lcys and LCHM are plotted in Fig. 1, respectively. The obvious absorption peaks of the Lcys could be seen located at 1.39, 1.70 and 2.82 THz, while more resonant absorption peaks of the LCHM are found at 1.15, 1.80, 2.24, 2.52, and 3.34 THz, respectively. It is known that many factors will contribute to the far-infrared terahertz response of the molecules, such as the chemical compositions and the structures of the molecules. Except for the different compositions of the chloride ion ($Cl^-$) and water molecules between the Lcys and the LCHM molecule, they also exhibit quite different molecular structures.

As depicted in Fig. 2(a) and (b), the 3D hydrogen-bond network of the Lcys lattice along *Z* and *Y* axis shows that the three-dimensional (3D) structure of the Lcys is formed by cysteine zwitterions (i.e., –$COO^-$/–$NH_3^+$), which interact mainly through intermolecular N–H···O hydrogen bonds and additional S–H···S hydrogen bonds [23]. The layers shown in Fig. 2(a) are connected by $N_1$–$H_6$···$O_2$ hydrogen bonds, and hydrogen-bonded layers in Fig. 2(b) are linked by $N_1$–$H_7$···$O_2$ and $N_1$–$H_5$···$O_1$ interactions. The hydrogen bond network of the LCHM is shown in Fig. 2(c) along *Z* axis and Fig. 2(d) along *X* axis, respectively. The –COOH group forms a hydrogen bond, $O_1$–$H_8$···$Cl_1$, with a chloride anion. The $NH_3^+$ group in the amino acid backbone forms three hydrogen bonds: two with water molecules and one with $Cl^-$. The water molecules act as hydrogen bond donors to form two O–H···Cl hydrogen bonds. The thiol group forms a long $S_1$–$H_7$···$Cl_1$ hydrogen bond. It is obvious that the LCHM crystal has a layered structure, with the amino acid –$CH_2$–SH side-chains arranged outside the layers. As a result, no

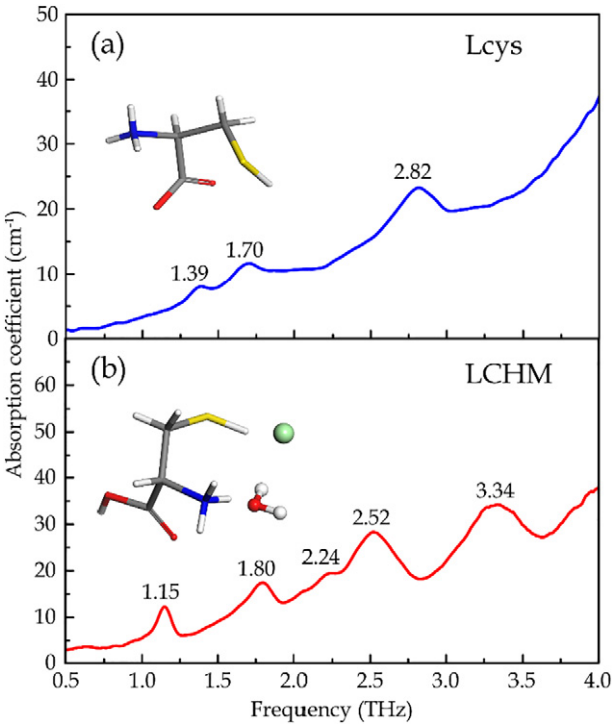


**Fig. 1.** The THz absorption coefficients of Lcys and LCHM at room temperature.

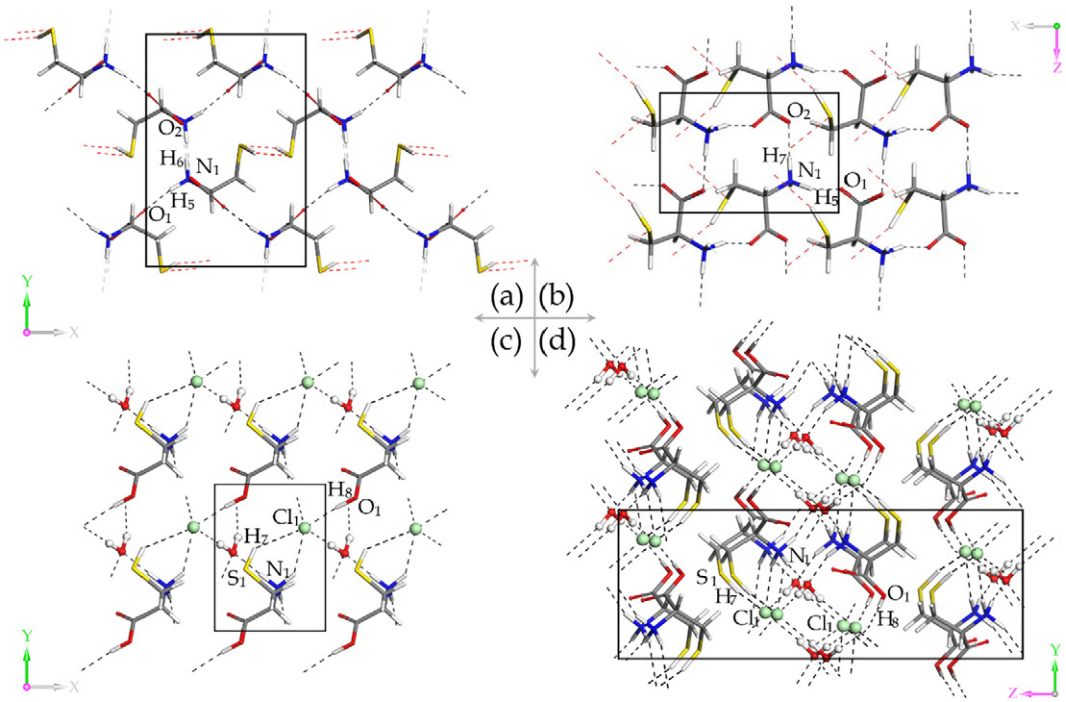


**Fig. 2.** The hydrogen-bond networks of Lcys (a) (b) and LCHM (c) (d).

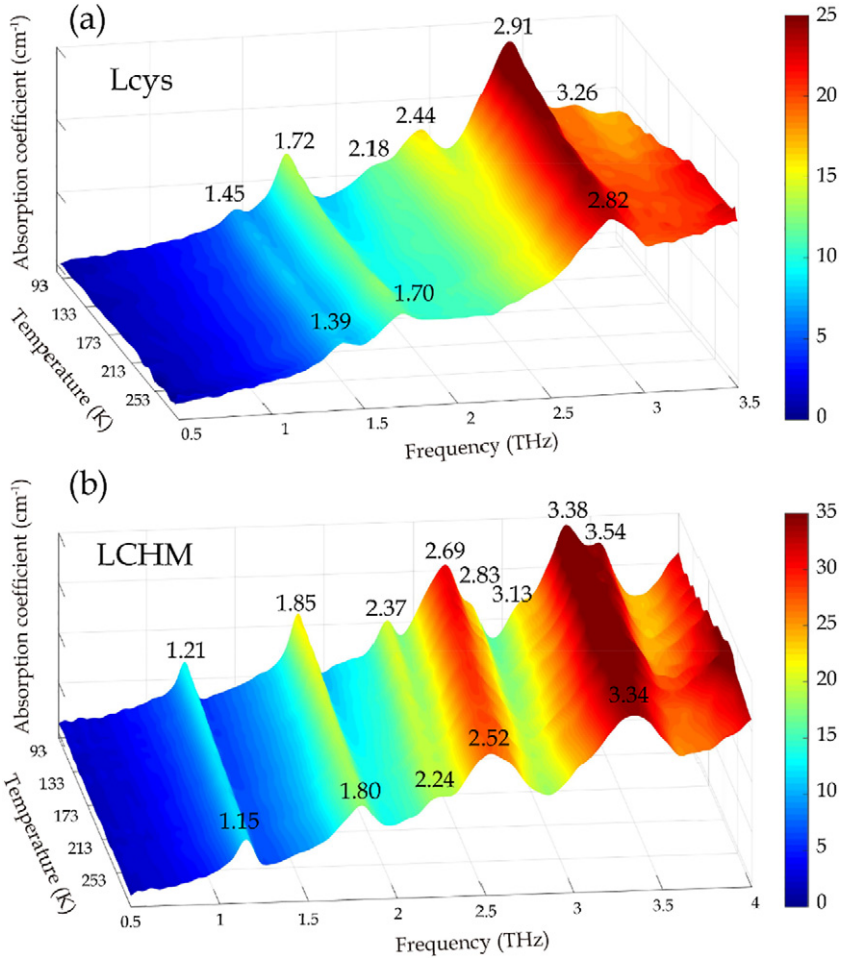


**Fig. 3.** Evolution of the THz absorption spectra of Lcys and LCHM from 83 to 293 K. (the color bar stands for the magnitude of absorption coefficient.)

hydrogen bonds exist between the layers [24]. Hydrogen-bond lengths of Lcys and LCHM can be found in Table S1 of Supplementary materials.

Many studies have indicated that terahertz spectroscopy is a powerful tool for detecting the weak bonding in crystals, including hydrogen bond [21,25,26]. Terahertz vibrational spectroscopy is sensitive to the intermolecular vibrations in crystals which usually contain the stretching of hydrogen bond. In this work, both Lcys and LCHM have distinctive hydrogen bond networks and the experimental THz absorbance could reveal these weak interactions. Furthermore, the quantum chemical calculations provide a reliable assignment of the observed THz spectra. Therefore, the highly sensitivity of terahertz spectroscopy to the molecular compositions and structures could provide fingerprints to identify the molecules.

### 4.2. Temperature effect on Lcys and LCHM

Furthermore, the temperature dependence of the terahertz power absorption of the Lcys and the LCHM are recorded over a temperature range of 83 to 293 K. As shown in Fig. 3, on cooling, because of vibrational anharmonicity, the terahertz absorption peaks become narrower, stronger, and slightly blue-shifted for both the Lcys and the LCHM sample. For the Lcys, the peaks at 1.39, 1.70 and 2.82 THz were blue shifted slightly to 1.45, 1.72 and 2.91 THz, respectively. Below 150 K, two inconspicuous absorption peaks at 2.18 and 2.44 THz at room-temperature become obvious and pronounced. Similarly, for LCHM, the peaks at 1.15, 1.80 and 2.24 THz were blue-shifted to 1.21, 1.85 and 2.37 THz. With temperature decrease, the peak at 2.52 THz splits into two peaks at 2.69 and 2.83 THz when the temperature is reduced to 83 K, and the peak at 3.34 THz also splits into two peaks at 3.38 and 3.54 THz. In fact, the temperature plays a very important role in revealing characteristic features of many weak vibrational modes of molecules that are weak or not observable at room temperature. As the temperature is decreased and more molecules populate the ground state, the average frequency of the absorption envelope would tend to increase [27].

### 4.3. Calculations

For a more quantitative analysis of the measured data, we perform the quantum chemical calculations based on the published database in CCDC (Cambridge Crystallographic Data Centre) and our PXRD measurements. Fig. 4(a) and (b) show the measured PXRD spectra of our samples, which are in agree very well with those calculated based on crystal cell parameters of the previous reports [9,23]. Fig. 4(c) and (d) show the crystal structures of Lcys and LCHM with the corresponding lattice parameters: (c) $a = 8.1109$ Å, $b = 12.1621$ Å, $c = 5.4210$ Å, $\alpha$, $\beta$, $\gamma = 90°$ for the Lcys, and $a = 5.4588$ Å, $b = 7.1570$ Å, $c = 19.389$ Å, $\alpha$, $\beta$, $\gamma = 90°$, for the LCHM, respectively. Both Lcys and LCHM are suggested to be orthorhombic in structure with non-centrosymmetric space group $P2_12_12_1$ ($Z = 4$).

The calculated and experimental THz spectra of Lcys and LCHM are plotted in Fig. 5, where the calculated results are overall in good agreement with the experimental ones. However, there are some offset and differences between simulations and experiments, which might be caused by disparity of crystal situations and temperature effect. To be specific, the simulations were performed on perfect crystal structure while it is hard to idealize in the actual experimental measurements, and the temperature difference between simulations (0 K) and experiments (83–293 K) could lead to shift and split of peak.

The distinctive vibrations in the THz region are described as intermolecular vibrations and molecular flexing [28], and the intermolecular vibrational modes are also related to hydrogen bond interactions [21,25,26]. For a clear identification of vibrational modes, six typical vibrational modes of Lcys and LCHM are demonstrated in Fig. 6(a–c) and (d–f) respectively. For Lcys, the experimental peak at 1.39 THz corresponds to the vibrational mode calculated at 1.59 THz, arising from collective vibration of the Lcys molecules. The measured peak at 1.70 THz is relative to the calculated peak at 1.80 THz, arising from the translational vibration of backbone, $-CH_2-SH$ side chain rotation and $-COO^-$ twisting. The measured feature at 2.82 THz is produced by the calculated mode at

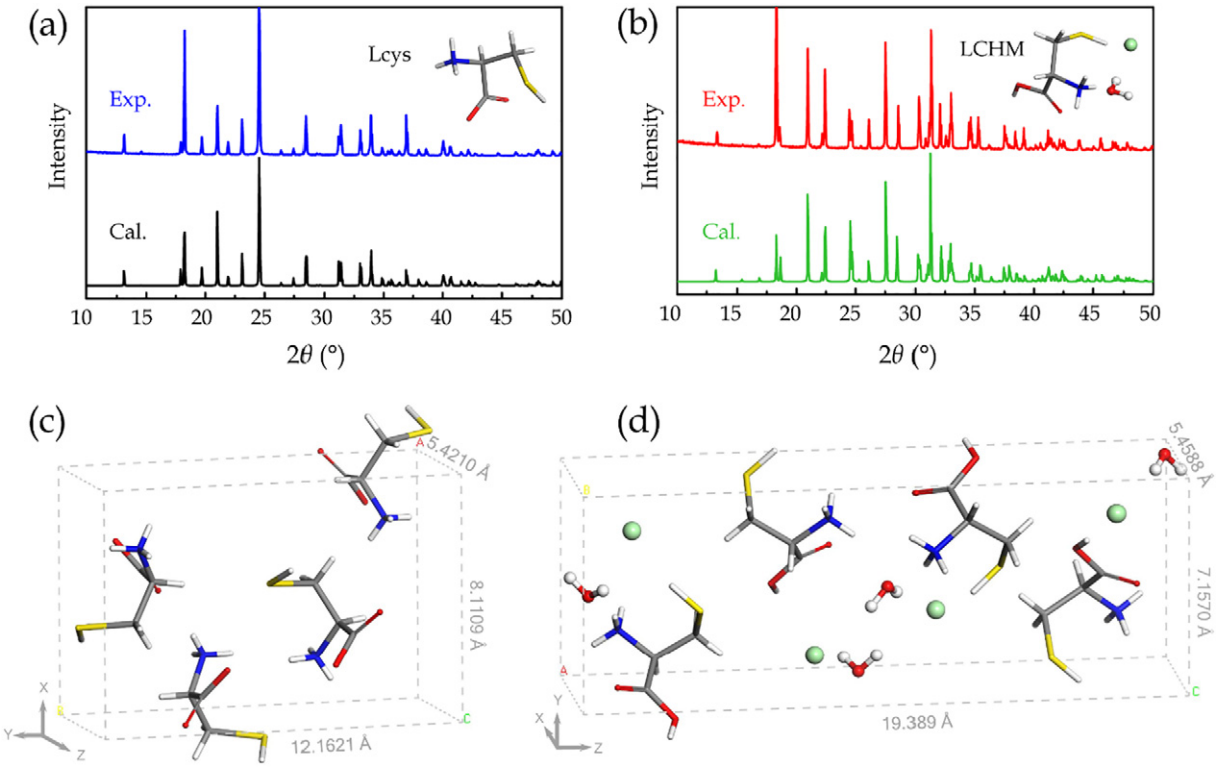


**Fig. 4.** The experimental and calculated PXRD patterns of (a) Lcys, (b) LCHM and the crystal structure for (c) Lcys and (d) LCHM.

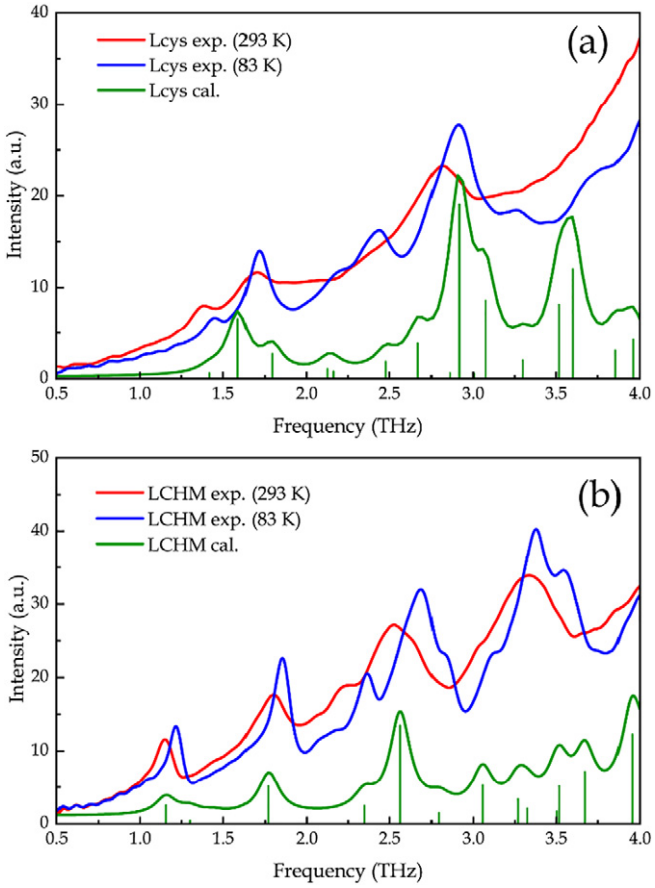


**Fig. 5.** The experimental and calculated spectra of Lcys (a) and LCHM (b).

2.92 THz, which primarily originates from translation of $-NH_3^+$ and wagging of $-COO^-$.

For LCHM, the experimental peak at 1.15 THz corresponds to the vibrational mode calculated at 1.16 THz, mainly from the $-CH_2-SH$ side chain, $-NH_3^+$ group translation and slight twisting of –COOH group. The 1.80 THz peak agrees with the calculated peak at 1.77 THz, arising from wagging of backbone, rotational vibration of –SH group and translation of $Cl^-$ and water molecule. The measured feature at 2.52 THz is relative to the simulated mode at 2.56 THz, which originates from wagging of entire amino acid chain and translation of $Cl^-$ and water molecule. The detailed descriptions of vibrational modes of Lcys and LCHM were presented in Table 1.

The DFT calculations result suggests that the characterized features of Lcys and LCHM in terahertz region mainly originate from collective vibrations of molecules and each feature corresponds to a specific vibrational mode. Incorporation of water molecules and chloride ions makes the lattice of LCHM completely different from Lcys in dimensions, symmetry and hydrogen bond distribution, and thus results in significant changes of intermolecular motions and terahertz spectra.

## 5. Conclusion

In conclusion, the far-infrared terahertz spectrum of the solid amino acid Lcys and its hydrochloride derivatives LCHM is dominated by the intermolecular vibrations. The temperature-dependent terahertz power absorptions of the Lcys and the LCHM show that they exhibit different terahertz response due to different intermolecular interactions, which are highly associated with the hydrogen-bond network. The DFT calculations provide clear evidence for the appearance of intermolecular vibrations of the Lcys and the LCHM in the far-infrared terahertz range, and indicate that the characterized features of Lcys and LCHM originate from effects of both hydrogen bonds and intermolecular interactions within the crystal lattice. The presented study here provides the basic spectral properties of the Lcys and LCHM in the far-infrared terahertz region and is helpful for ones to understand the low-frequency vibrations of amino acid.

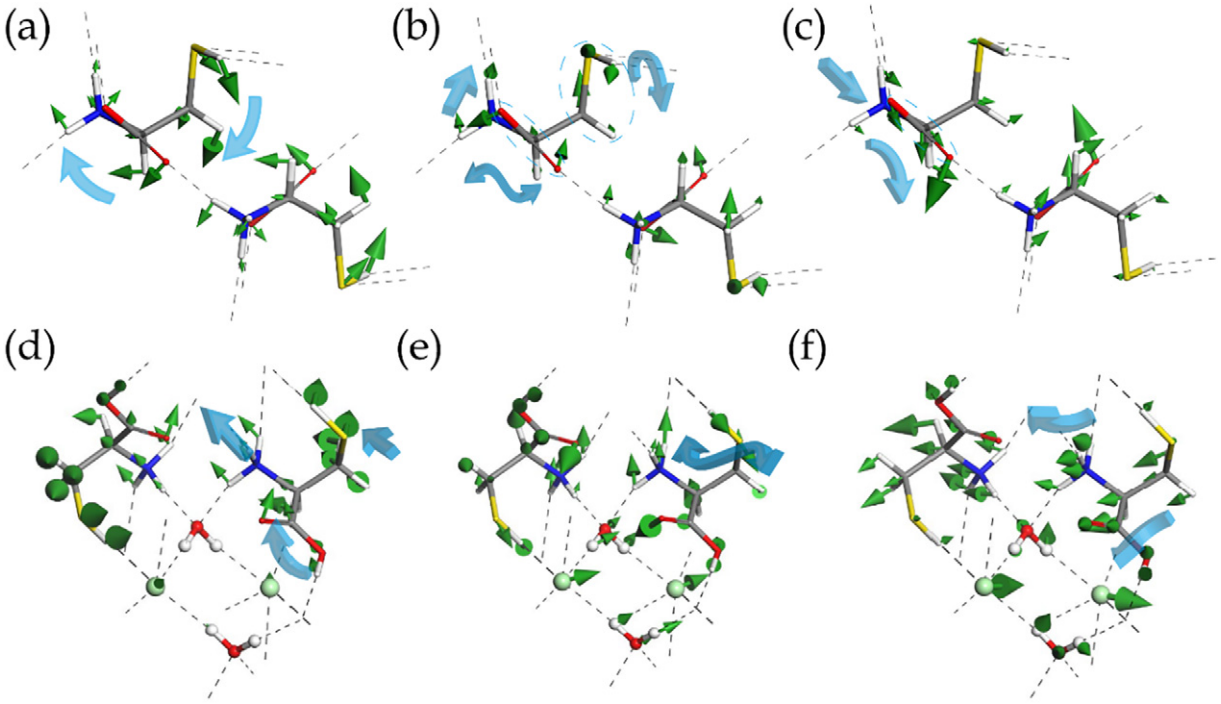


**Fig. 6.** The calculated vibrational modes of Lcys at (a) 1.59, (b) 1.80, (c) 2.92 THz, and LCHM at (d) 1.16, (e) 1.77, (f) 2.56 THz, respectively. Corresponding animations can be found in Supplementary materials.

**Table 1**
The absorption peaks and the corresponding vibrational modes of Lcys and LCHM.

| Compound | Exp. (THz) | | Cal. (THz) | Vibrational mode description[a] |
|---|---|---|---|---|
| | 293 K | 83 K | | |
| Lcys | 1.39 | 1.45 | 1.59 | Collective |
| | | 1.72 | 1.80 | $t$(backbone), $\rho$(–$CH_2$–SH) and $\tau$(–$COO^-$) |
| | 1.70 | 2.18 | 2.13 | Collective |
| | | | 2.16 | $t$(backbone), $\tau$(–$COO^-$) and $\nu$(N1–H6···O2) |
| | | 2.44 | 2.48 | Collective, $\nu$(S1–H1···S1) |
| | | | 2.67 | $b$(backbone), $\nu$(N1–H5···O1) |
| | | 2.91 | 2.92 | $t$(–$NH_3^+$), $\omega$(–$COO^-$) and $\nu$(N1–H5···O1) |
| | | | 3.08 | Collective |
| | 2.82 | | 3.30 | Collective, $\nu$(N1–H7···O2) |
| | | 3.26 | 3.52 | $\rho$(backbone), $t$(–$NH_3^+$) and $\nu$(N1–H6···O2) |
| | | | 3.60 | Mainly from $\rho$(–$CH_2$–SH), $\nu$(S1–H1···S1) |
| LCHM | 1.15 | 1.21 | 1.16 | $t$(–$CH_2$–SH), $t$(–$NH_3^+$) and $\tau$(–COOH) |
| | 1.80 | 1.85 | 1.77 | $\omega$(backbone), $\rho$(–SH), $t$($Cl^-$) and $t$($H_2O$) |
| | 2.24 | 2.37 | 2.35 | $\rho$(–SH), $\omega$(backbone) |
| | | 2.69 | 2.56 | $\omega$ (backbone), $t$($Cl^-$) and $t$($H_2O$) with $\nu$($O1^W$–$H1^W$···Cl) |
| | 2.52 | 2.83 | 2.79 | $\omega$(backbone), $\rho$(–SH), $t$($Cl^-$) and $t$($H_2O$) |
| | | | 3.06 | $\omega$(–COOH), $t$(–SH), $t$($Cl^-$) and $\nu$(O1–H8···Cl) |
| | | 3.13 | 3.27 | $\rho$(backbone), $t$($Cl^-$) and $t$($H_2O$) with $\nu$(O1–H8···Cl) |
| | | 3.38 | 3.32 | $\omega$(–COOH), $t$(–SH) and $\nu$(N1–H4···$O1^W$) |
| | 3.34 | 3.54 | 3.52 | $\rho$(–$CH_2$–SH), $t$(–COOH), $t$($Cl^-$) and $\nu$(S1–H7···Cl1) |

[a] The abbreviations employed for vibrations are: $t$ (translation), $\omega$ (wagging), $\rho$ (rotation), $\nu$(stretching), $b$ (bending) and $\tau$ (twisting); numbering schemes of Lcys and LCHM are presented in Supplementary data.

## Acknowledgements

This work was supported by the National Key Research and Development Program of China (with grant NO. 2017YFA0701004), the National Science Foundation of China (Grant Nos. 61875150, 61605143, 61735012, 61420106006, 61722509 and 61871212), and the National Defence Science and Technology Innovation Special Zone.

## Appendix A. Supplementary data

Supplementary data to this article can be found online at https://doi.org/10.1016/j.saa.2019.117476.

## References

[1] C.N. Pace, G.R. Grimsley, J.M. Scholtz, Protein ionizable groups: pK values and their contribution to protein stability and solubility, J. Biol. Chem. 284 (2009) 13285–13289, https://doi.org/10.1074/jbc.R800080200.
[2] Z.R. Zhang, G. Cui, X. Liu, et al., Determination of the functional unit of the cystic fibrosis transmembrane conductance regulator chloride channel. One polypeptide forms one pore, J. Biol. Chem. 280 (2005) 458–468https://doi.org/10.1074/jbc.M409626200.
[3] A. Cossaro, S. Terreni, O. Cavalleri, et al., Electronic and geometric characterization of the L-cysteine paired-row phase on Au(110), Langmuir 22 (2006) 11193–11198https://doi.org/10.1021/la061833r.
[4] M.H. Stipanuk, J.E. Dominy Jr., J.I. Lee, et al., Mammalian cysteine metabolism: new insights into regulation of cysteine metabolism, J. Nutr. 136 (2006) 1652S–-1659Shttps://doi.org/10.1093/jn/136.6.1652S.
[5] D.B. Simon, R.S. Bindra, T.A. Mansfield, et al., Mutations in the chloride channel gene, CLCNKB, cause Bartter's syndrome type III, Nat. Genet. 17 (1997) 171https://doi.org/10.1038/ng1097-171.
[6] A. Finch, D.A. Ledward. A differential scanning calorimetric study of cysteine hydrochloride monohydrate. Thermochim. Acta 11 (1975), 157–161, https://doi.org/10.1016/0040-6031(75)80019-0.
[7] R. Schillinger, Z. Sljivancanin, B. Hammer, et al., Probing enantioselectivity with x-ray photoelectron spectroscopy and density functional theory, Phys. Rev. Lett. 98 (2007) 136102, https://doi.org/10.1103/PhysRevLett.98.136102.
[8] V.S. Min'kov, Y.A. Chesalov, E.V. Boldyreva, Study of the temperature effect on IR spectra of crystalline amino acids, dipeptides, and polyamino acids. IV. L-cysteine and DL-cysteine, J. Struct. Chem. 49 (2008) 1022–1034https://doi.org/10.1007/s10947-008-0174-5.
[9] R.P. Chapman, D.L. Bryce, A high-field solid-state 35/37Cl NMR and quantum chemical investigation of the chlorine quadrupolar and chemical shift tensors in amino acid hydrochlorides, Phys. Chem. Chem. Phys. 9 (2007) 6219–6230https://doi.org/10.1039/B712688C.
[10] G. Bhagavannarayana, S. Kumar, M. Shakir, et al., Unidirectional growth of L-cysteine hydrochloride monohydrate: first time observation as nonlinear optical material and its characterization, J. Appl. Crystallogr. 43 (2010) 710–715https://doi.org/10.1107/S0021889810016870.
[11] L. Ho, M. Pepper, P. Taday, Terahertz spectroscopy: signatures and fingerprints, Nat. Photonics 2 (2008) 541, https://doi.org/10.1038/nphoton.2008.174.
[12] M. Janek, D. Zich, M. Naftaly, Terahertz time-domain spectroscopy response of amines and amino acids intercalated smectites in far-infrared region, Mater. Chem. Phys. 145 (2014) 278–287https://doi.org/10.1016/j.matchemphys.2014.02.004.
[13] P.C. Upadhya, Y.C. Shen, A.G. Davies, et al., Far-infrared vibrational modes of polycrystalline saccharides, Vib. Spectrosc. 35 (2004) 139–143https://doi.org/10.1016/j.vibspec.2003.12.010.
[14] J. Kröll, J. Darmo, K. Unterrainer, Terahertz optical activity of sucrose single-crystals, Vib. Spectrosc. 43 (2007) 324–329https://doi.org/10.1016/j.vibspec.2006.03.010.
[15] F. D'Angelo, Z. Mics, M. Bonn, et al., Ultra-broadband THz time-domain spectroscopy of common polymers using THz air photonics, Opt. Express 22 (2014) 12475–12485https://doi.org/10.1364/OE.22.012475.
[16] S.J. Clark, M.D. Segall, C.J. Pickard, et al., First principles methods using CASTEP, Z. Krist. Cryst. Mater. 220 (2005) 567–570https://doi.org/10.1524/zkri.220.5.567.65075.
[17] J.P. Perdew, K. Burke, M. Ernzerhof, Generalized gradient approximation made simple, Phys. Rev. Lett. 77 (1996) 3865–3868https://doi.org/10.1103/PhysRevLett.77.3865.
[18] S. Grimme, Semiempirical GGA-type density functional constructed with a long-range dispersion correction, J. Comput. Chem. 27 (2006) 1787–1799https://doi.org/10.1002/jcc.20495.
[19] Z. Xu, X. Lv, J. Chen, et al., Dispersion-corrected DFT investigation on defect chemistry and potassium migration in potassium-graphite intercalation compounds for potassium ion batteries anode materials, Carbon 107 (2016) 885–894https://doi.org/10.1016/j.carbon.2016.06.101.
[20] H. Fang, M.T. Dove, K. Refson, Ag–Ag dispersive interaction and physical properties of Ag 3 Co (CN) 6, Phys. Rev. B 90 (2014), 054302. https://doi.org/10.1103/PhysRevB.90.054302.
[21] M. Takahashi, Terahertz vibrations and hydrogen-bonded networks in crystals, Crystals 4 (2014) 74–103https://doi.org/10.3390/cryst4020074.
[22] L. Duvillaret, F. Garet, J.-L. Coutaz, Highly precise determination of optical constants and sample thickness in terahertz time-domain spectroscopy, Appl. Opt. 38 (1999) 409–415https://doi.org/10.1364/AO.38.000409.
[23] S.A. Moggach, D.R. Allan, S.J. Clark, et al., High-pressure polymorphism in L-cysteine: the crystal structures of L-cysteine-III and L-cysteine-IV, Acta Crystallogr. B 62 (2006) 296–309, https://doi.org/10.1107/S0108768105038802.
[24] V.V. Ghazaryan, V.S. Minkov, E.V. Boldyreva, et al., L-cysteine halogenides: a new family of salts with an L-cysteine···L-cysteinium dimeric cation, J. Mol. Struct. 1121 (2016) 60–69https://doi.org/10.1016/j.molstruc.2016.05.049.
[25] B.M. Fischer, H. Helm, P.U. Jepsen, Chemical recognition with broadband THz spectroscopy, Proc. IEEE 95 (2007) 1592–1604https://doi.org/10.1109/JPROC.2007.898904.
[26] A. Matei, N. Drichko, B. Gompf, et al., Far-infrared spectra of amino acids, Chem. Phys. 316 (2005) 61–71https://doi.org/10.1016/j.chemphys.2005.04.033.
[27] A. Xie, Q. He, L. Miller, et al., Low frequency vibrations of amino acid homopolymers observed by synchrotron far-IR absorption spectroscopy: excited state effects dominate the temperature dependence of the spectra, Biopolymers 49 (1999) 591–603, https://doi.org/10.1002/(SICI)1097-0282(199906)49:7<591::AID-BIP5>3.0.CO;2-Q.
[28] A.C. Jørgensen, C.J. Strachan, K.H. Pöllänen, et al., An insight into water of crystallization during processing using vibrational spectroscopy, J. Pharm. Sci. 98 (2009) 3903–3932https://doi.org/10.1002/jps.21735.